Assessment of Roles of Surface Histidyl Residues in the Molecular Basis of the Bohr Effect and of β143 Histidine in the Binding of 2,3-Bisphosphoglycerate in Human Normal Adult Hemoglobin†

Tsuei-Yun Fang, Ming Zou, Virgil Simplaceanu, Nancy T. Ho, and Chien Ho*

Department of Biological Sciences, Carnegie Mellon University, 4400 Fifth Avenue, Pittsburgh, Pennsylvania 15213

Received May 18, 1999; Revised Manuscript Received July 27, 1999

ABSTRACT: Site-directed mutagenesis has been used to construct two mutant recombinant hemoglobins (rHbs), rHb(βH116Q) and rHb(βH143S). Purified rHbs were used to assign the C2 proton resonances of β116His and β143His and to resolve the ambiguous assignments made over the past years. In the present work, we have identified the C2 proton resonances of two surface histidyl residues of the β chain, β116His and β143His, in both the carbonmonoxy and deoxy forms, by comparing the proton nuclear magnetic resonance (NMR) spectra of human normal adult hemoglobin (Hb A) with those of rHbs. Current assignments plus other previous assignments complete the assignments for all 24 surface histidyl residues of human normal adult hemoglobin. The individual p*K* values of 24 histidyl residues of Hb A were also measured in deuterium oxide (D_2O) in 0.1 M *N*-(2-hydroxyethyl)piperazine-*N*′-2-ethanesulfonic acid (HEPES) buffer in the presence of 0.1 M chloride at 29 °C by monitoring the shifts of the C2 proton resonances of the histidyl residues as a function of pH. Among those surface histidyl residues, β146His has the biggest contribution to the alkaline Bohr effect (63% at pH 7.4), and β143His has the biggest contribution to the acid Bohr effect (71% at pH 5.1). α20His, α112His, and β117His have essentially no contribution; α50His, α72His, α89His, β97His, and β116His have moderate positive contributions; and β2His and β77His have a moderate negative contribution to the Bohr effect. The sum of the contributions from 24 surface histidyl residues accounted for 86% of the alkaline Bohr effect at pH 7.4 and about 55% of the acid Bohr effect at pH 5.1. Although β143His is located in the binding site for 2,3-bisphosphoglycerate (2,3-BPG) according to the crystal structure of deoxy-Hb A complexed with 2,3-BPG, β143His is not essential for the binding of 2,3-BPG in the neutral pH range according to the proton NMR and oxygen affinity studies presented here. With the accurately measured and assigned individual p*K* values for all surface histidyl residues, it is now possible to evaluate the Bohr effect microscopically for novel recombinant Hbs with important functional properties, such as low oxygen affinity and high cooperativity. The present study further confirms the importance of a global electrostatic network in regulating the Bohr effect of the hemoglobin molecule.

The oxygenation of the hemoglobin (Hb)[1] molecule is regulated both by interactions among its oxygen-binding sites (homotropic interactions) and by interactions between individual amino acid residues and various solutes (heterotropic interactions). Heterotropic effectors include the hydrogen ion, chloride, inorganic phosphate, and 2,3-bisphosphoglycerate (2,3-BPG) (*1*−*3*). The effect of pH on the oxygen affinity of Hb is known as the Bohr effect. Below pH 6.5, the oxygen affinity increases as the concentration of hydrogen ions increases (the acid Bohr effect); above pH 6.5, the oxygen affinity increases as the concentration of hydrogen ions decreases (the alkaline Bohr effect) (*4*, *5*).

The Bohr effect, usually expressed as the number of hydrogen ions released upon oxygenation, can be measured by two independent methods. First, it can be determined directly from the titration of H^+ ions released or taken up by Hb on oxygen (or CO) binding. Second, it can be determined from the change in oxygen affinity as a function of pH. According to Wyman's linkage model (*5*), there is an exact relationship between the change of oxygen affinity and the number of H^+ ions released or taken up as a function of pH. This macroscopically measured Bohr effect is a summation of the effects of changes in the H^+ affinity upon oxygenation of the Hb molecule. The molecular basis of the Bohr effect is the change of dissociation constant of specific H^+ binding sites upon oxygenation. Any amino acid residue that changes its p*K* value between the deoxy and oxy (or CO) forms of the Hb molecule participates in the Bohr effect. Some amino acid residues that have differential affinities for anions between the deoxy and oxy (or CO) states are also potential Bohr groups (*3*, *6*−*8*).

Considerable experimental and theoretical studies during the past three decades have been devoted to identifying those

† This work is supported by a research grant from the National Institutes of Health (HL-24525).

* Address correspondence to this author: telephone 412-268-3395; FAX 412-268-7083; E-mail chienho@andrew.cmu.edu.

[1] Abbreviations: Hb A, human normal adult hemoglobin; rHb, recombinant hemoglobin; NMR, nuclear magnetic resonance; ppm, parts per million; DSS, 2,2-dimethyl-2-silapentane-5-sulfonate; HEPES, *N*-(2-hydroxyethyl)piperazine-*N*′-2-ethanesulfonic acid; Bis-Tris, bis(2-hydroxyethyl)iminotris(hydroxymethyl)methane; 2,3-BPG, 2,3-bisphosphoglycerate; 2D, two-dimensional; TOCSY, total correlation spectroscopy.

10.1021/bi9911379 CCC: $18.00
Published on Web 09/14/1999

amino acid residues whose p*K* values change between the deoxy and oxy (or CO) states (*3, 6*−*18*). The side chains of histidyl residues have intrinsic p*K* values in the physiological pH range. They are the likely sites for H^+ binding (or release) when the Hb molecule undergoes conformational changes in going from the deoxy to the oxy state. There are 10 and nine histidyl residues in the α- and β-chains of human normal adult hemoglobin (Hb A), respectively (*19*). Among them, α20His, α50His, α72His, α89His, α112His, β2His, β77His, β97His, β116His, and β117His are on the surface of the Hb A molecule. β143His is partially exposed to solvent in the central cavity of the Hb A molecule. β146His participates in salt-bridge formation in the deoxy form of Hb A and is partially exposed to solvent upon oxygenation (*20, 21*). These surface histidyl residues (including β143His and β146His) are likely to be involved in the Bohr effect.

Proton nuclear magnetic resonance (NMR) spectroscopy is particularly suited for studying the involvement of histidyl residues in the Bohr effect because the C2 ($C_{\epsilon 1}$) proton resonances of the histidyl residues usually are resolved from other proton resonances. Extensive NMR spectroscopic studies on resonances arising from the C2 protons of histidyl residues have been conducted in our laboratory (*3, 6*−*8, 10, 11, 16*−*18, 22*). These C2 proton resonances have been labeled with the letters A, B, ..., L, and Y in the CO form, and with numbers 1, 2, ..., 10 in the deoxy form (see Figures 2 and 5). Many resonance assignments of surface histidyl residues have been made using naturally occurring mutant Hbs or chemically modified Hbs or recombinant mutant Hbs (for a summary of historical assignments of C2 proton resonances, see ref *18*). The assignments for several surface histidyl residues, however, either have not been determined or the assignments have been controversial. A previous study on Hb A_2 (*11*) has assigned resonances J, K, 7, and 8 to β116 and β117 histidine residues; however, the individual assignments for these two histidyl residues have not been specified. The assignments for β97His and β143His have been controversial. The previous tentative assignment for β143His in deoxy form, resonance 9, has been reassigned to α89His in recent studies (*10, 18*). Resonance C has been assigned to β97His by using Hb Malmö (βH97Q) and Hb Wood (βH97L) (*13, 15*). However, resonance C is also missing in the proton NMR spectra of Hb des-His (β146His deleted), Hb Barcelona (βD94H), and Hb Abruzzo (βH143R) (*16*). Similarly, resonance L is missing in the proton NMR spectra of Hb Abruzzo (βH143R), Hb des-His (β146His deleted), and Hb Barcelona (βD94H) (*16*). Although the finding that resonance L is broadened in the presence of 2,3-BPG suggests that it arises from β143His, no conclusive assignment for resonance L has been made (*3, 22*).

2,3-BPG is a heterotropic effector of Hbs and a predominant phosphorylated metabolite inside red blood cells (*1, 23*). The binding of 2,3-BPG leads to a dramatic decrease in the oxygen affinity of the Hb molecule and thus facilitates the unloading of oxygen to the tissues (*1, 23*). According to the crystal structure of deoxy-Hb A complexed with 2,3-BPG, 2,3-BPG forms salt bridges with N-terminal amino groups, His2 and His143 of both β-chains, and with Lys82 of one β-chain (*24*). ^{31}P NMR studies also suggest that 2,3-BPG binds to the same residues in oxy-Hb A (*25*). 2,3-BPG binds less well to fetal hemoglobin (Hb F) than to Hb A. Hb F consists of two α-chains and two γ-chains, instead of two α-chains and two β-chains (*19*). The amino acid sequences of β-chains and γ-chains are different at 39 positions. One of the differences in the amino acid sequence between β- and γ-chains is that position 143 (H21) is a histidine in the β-chain and is the uncharged serine in the γ-chain (*19*).

In this study, we have attempted to complete and to confirm the resonance assignments of the surface histidyl residues in the Hb A molecule. In addition to the resonance assignments, the role of β143His in the binding of 2,3-BPG is also investigated. Two mutant recombinant hemoglobins (rHbs), rHb(βH116Q) and rHb(βH143S), have been constructed and expressed in *Escherichia coli*. By comparing the C2 proton resonances of the histidyl residues of the rHbs with those of Hb A, the C2 proton resonances of β116His and β143His have been identified. The assignment of β116His leads to the assignment for β117His indirectly. The assignment of β143His also clarifies the ambiguity of the assignment for β97His. The individual p*K* values of 24 histidyl residues of Hb A were measured in D_2O in 0.1 M HEPES buffer plus 0.1 M chloride. With these p*K* values and the oxygen dissociation data that were also measured in D_2O in 0.1 M HEPES buffer plus 0.1 M chloride, we have calculated the contributions of individual surface histidyl residues to the Bohr effect. The sum of the contributions from the assigned 24 surface histidyl residues account for 86% of the alkaline Bohr effect at pH 7.4 and 55% of the acid Bohr effect at pH 5.1. The ^1H NMR studies and oxygen affinity data both have shown that rHb(βH143S) is affected by 2,3-BPG and imply that 2,3-BPG also binds to rHb(βH143S).

MATERIALS AND METHODS

Materials. The expression vector pHE2, containing synthetic α- and β-globin genes and the *E. coli* methionine aminopeptidase gene, was constructed in a previous study to produce recombinant Hb A (*26*). The Altered Sites II in vitro mutagenesis system was from Promega. The Muta-Gene Phagemid in vitro mutagenesis kit was from Bio-Rad. T4 DNA ligase, polynucleotide kinase, and restriction enzymes were from Boehringer Mannheim or Promega. Synthetic oligonucleotides were from DNA International. Q-Sepharose fast-flow, Sephadex G-25, and the Mono-S column were from Pharmacia. [1,3-^{13}C(99%)]Glycerol and D_2O (99.9% in deuterium content) were from Cambridge Isotope Laboratories. Bis(2-hydroxyethyl)iminotris(hydroxymethyl)methane (Bis-Tris) was from Aldrich. *N*-(2-Hydroxyethyl)piperazine-*N*′-2-ethanesulfonic acid (HEPES) and its sodium salt were from Sigma.

Site-Directed Mutagenesis. The synthetic human normal β-globin gene was mutated according to the protocols of the Altered Sites II in vitro mutagenesis system and the Muta-Gene Phagemid in vitro mutagenesis kit for rHbs(βH116Q) and rHb(βH143S), respectively. The mutated β-globin genes were then used to replace the human normal β-globin gene in pHE2 to construct expression vectors pHE2006 and pHE270 for rHbs(βH116Q) and rHb(βH143S), respectively. The desired mutations were confirmed by DNA sequencing, which was done in the Biotechnology Center of the University of Pittsburgh.

Expression of Mutant rHbs. The expression vectors pHE2006 and pHE270 were individually transformed into

E. coli strain JM109. The transformed *E. coli* cells were grown in Terrific Broth (TB) medium plus 100 μg/mL ampicillin in a 10-L Microferm fermentor (New Brunswick Scientific, model BioFlow 3000) at 30−32 °C until the optical density at 600 nm reached 10. Then, isopropyl 1-thio-β-D-galactopyranoside was added to a final concentration of 0.1 mM to induce the expression of mutant rHbs and of methionine aminopeptidase. The culture was supplemented with hemin (50 mg/L) and was grown for an additional 4−5 h. Cells were harvested by centrifugation and stored at −80 °C until purification.

Purification of Hb A and Mutant rHbs. Hb A was prepared and purified by standard procedures used in our laboratory (*27*). Mutant rHbs were prepared and purified by using high-pressure homogenization (Model EmulsiFlex-C5, Avestin), ultrafiltration concentration, poly(ethylenimine) precipitation, Q-Sepharose fast-flow column chromatography, an oxidation−reduction process, and Mono-S FPLC chromatography as described elsewhere (*26, 28−30*). The purified Hb A and rHbs [2−8% (w/v)], which were in the CO form, were added drop by drop into liquid nitrogen to make frozen Hb beads. The frozen Hb beads were stored at −80 °C.

Characterization of Mutant rHbs. To analyze the N-terminal residue, automated cycles of Edman degradation were performed with an Applied Biosystems gas−liquid-phase sequencer (Model 470/900A) equipped with an on-line phenylthiohydantoin amino acid analyzer (Model 120A). The electrospray ionization mass spectrometric analyses were performed on a VG Quattro-BQ (Fisons Instruments, VG Biotech, Altrincham, U.K.). These analyses were described previously (*18, 26, 28−30*).

Oxygen-Binding Measurements of Hb Samples. The oxygen dissociation curves of Hb A and rHbs were measured by a Hemox-Analyzer (TCS Medical Products, Huntington Valley, PA) at 29 °C as previously described (*30, 31*). HEPES buffer (0.1 M) plus 0.1 M chloride in D_2O and 0.1 M sodium phosphate buffer were used in this study. The methemoglobin (met-Hb) reductase system was used if needed to reduce the amount of met-Hb in the sample (*32*). Partial oxygen pressure at 50% saturation (P_{50}) and the Hill coefficient (n_{max}) were determined from each oxygen dissociation curve [for details, see Tsai et al. (*31*)]. The accuracy for P_{50} measurements (in millimeters of mercury) is ±5% and that for n_{max} is ±7%.

NMR Sample Preparation. HbCO (Hb in CO form) solutions and deoxy-Hb solutions were prepared as described elsewhere (*3, 6−8, 10, 11, 16, 18*). To maintain a constant chloride concentration in Hb samples, the pH values of Hb samples in 0.1 M HEPES buffer in D_2O (with or without chloride) were determined from the ^{13}C NMR chemical shift of the buffer carbons relative to the internal [1,3-^{13}C(99%)]-glycerol standard to avoid the chloride efflux from the pH electrode as described previously (*8*). However, when the pH value is less than 6.3, the pH values determined from ^{13}C NMR spectra are not very accurate. We measured the pH values of these low pH samples by pH meter right after the NMR experiments and then these Hb samples were discarded.

NMR Measurements. The ^1H NMR experiments were performed at 29 °C on Bruker Avance-DRX 300, 500, and 600 NMR spectrometers operating at 300.13, 500.13, and 600.13 (or 600.33) MHz, respectively. The ^{13}C NMR spectra were obtained at 29 °C at 75.04, 125.04, and 150.04 (or 150.08) MHz, respectively. The ^1H NMR spectra of Hbs in H_2O were obtained by using a jump-and-return pulse sequence (*33*) with a delay time of 1.0 s. The ^1H NMR spectra of Hbs in D_2O were obtained by using a single 90° pulse and a delay time of 1.0 s. Two-dimensional (2D) homonuclear total correlation spectroscopy (TOCSY) spectra were recorded by using the MLEV-17 sequence for mixing (*34*) and a delay time of 1.0 s. A total of 256−1024 transients were accumulated for each spectrum. Proton chemical shifts were referenced to the methyl proton resonance of 2,2-dimethyl-2-silapentane-5-sulfonate (DSS) indirectly. The water signal (H_2O) in the H_2O samples and the residual water signal (HDO) in D_2O samples, which occur at 4.76 ppm downfield from that of DSS at 29 °C, were used as the internal reference.

The p*K* values of the histidyl residues were determined by a nonlinear least-squares fit of the chemical shift of each C2 proton resonance, δ, as a function of pH (pH 4−9) according to

$$\delta = (\delta^+[H^+] + \delta^0 K)/([H^+] + K) \quad (1)$$

or

$$\delta = (\delta^+[H^+]^n + \delta^0 K^n)/([H^+]^n + K^n) \quad (2)$$

where δ^+ and δ^0 are the chemical shifts in the protonated and unprotonated forms of the histidyl residue, respectively, K is the H^+ dissociation equilibrium constant of the histidyl residue, and n is the titration coefficient for the ^1H NMR titration of the histidyl residue.

RESULTS

N-Terminal Analysis and Mass Spectrometry of Purified rHbs. To confirm the efficient cleavage of the N-terminal methionine residues of the purified rHbs, N-terminal analysis and mass spectrometry have been applied to the purified rHbs. The N-terminal analysis of purified rHbs by Edman degradation shows that at least 98% of either the α- or the β-chains of purified rHbs have valine as the N-terminal residue. Only a small percentage (2% at most) of the purified rHbs retain the methionine on the N-terminal. The molecular masses of purified rHbs as determined by electrospray ionization mass spectrometry are consistent with the calculated masses of these rHbs with the desired mutations and without the N-terminal methionine.

^1H NMR Studies of the Structural Features of rHbs. ^1H NMR spectroscopy has been an excellent tool to study the tertiary and quaternary structures of Hbs. Figure 1A shows the exchangeable proton resonances of HbCO A, rHbCO (βH116Q), and rHbCO (βH143S). The exchangeable proton resonances of the mutant rHbs that arise from the exchangeable protons in the subunit interface have no noticeable differences compared to those of Hb A. The subunit interfaces of Hb A are not affected by these two mutations on the surface of the β-chain. Figure 1B shows the ring-current shifted proton resonances of HbCO A, rHbCO (βH116Q), and rHbCO (βH143S). The ring-current shifted resonances are sensitive to the heme conformation and the tertiary structure in the heme pockets (*35*). The ring-current shifted resonances of rHbCO (βH143S) are essentially the

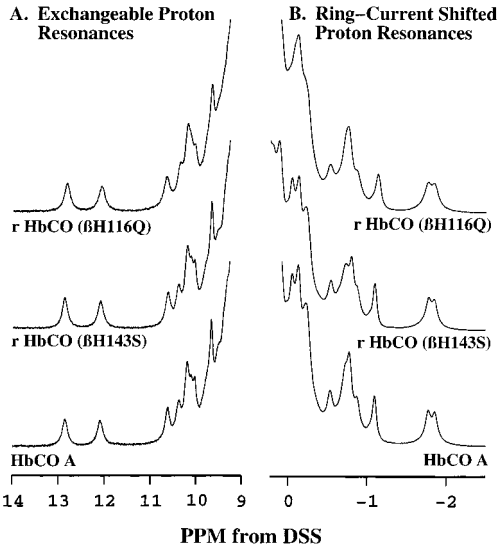

FIGURE 1: ^{1}H NMR spectra (300 MHz) of 4−6% solutions of rHbCO (βH116Q), rHbCO (βH143S), and HbCO A in H2O in 0.1 M sodium phosphate at pH 7.0 and 29 °C: (A) exchangeable proton resonances and (B) ring-current shifted proton resonances.

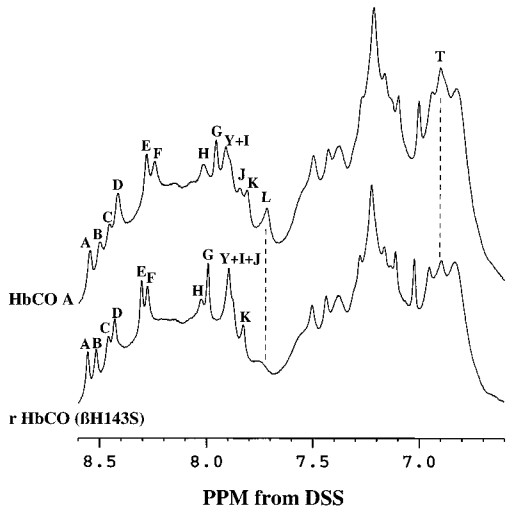

FIGURE 2: ^{1}H NMR spectra (300 MHz) of 4−6% solutions of rHbCO (βH143S) and HbCO A in D_2O in 0.1 M Bis-Tris at pH 6.6 and 29 °C.

same as those of HbCO A, while those of rHbCO (βH116Q) differ slightly from those of HbCO A. These differences imply slight adjustments of the heme conformation and/or the amino acid residues in the heme pockets due to the mutation. Previous studies have shown that such minor differences in the ring-current shifted resonances are common features in many mutant rHbs that we have studied (*18, 28*−*30*).

Assignment of the C2 Resonances of β116His and β143His in HbCO A. The C2 ($C_{\epsilon 1}$) and C4 ($C_{\delta 2}$) proton resonances (∼8.8−7.6 ppm and ∼7.6−6.4 ppm from DSS, respectively) of the histidyl residues of rHbCO (βH143S) and HbCO A in D_2O in 0.1 M Bis-Tris buffer at 29 °C are shown in Figure 2. Resonance L is missing in the region of C2 proton resonances in the spectrum of rHbCO (βH143S). We have also confirmed that resonance L is missing in other buffer conditions, such as phosphate and HEPES buffers at several different pH values (results not shown). These results have led to the assignment of C2 proton resonance L to β143His. Since the assignment for β143His has been controversial for

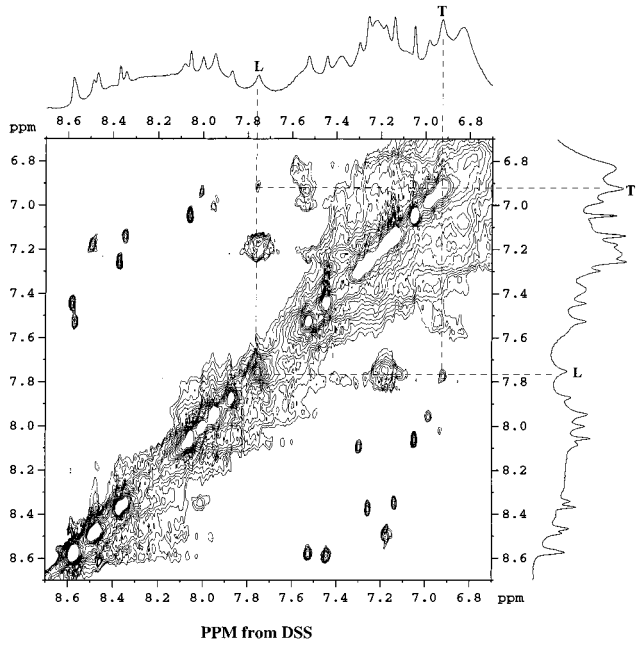

FIGURE 3: ^{1}H NMR TOCSY spectrum (300 MHz) of a 6% solution of HbCO A in D_2O in 0.1 M Bis-Tris at pH 6.4 and 29 °C.

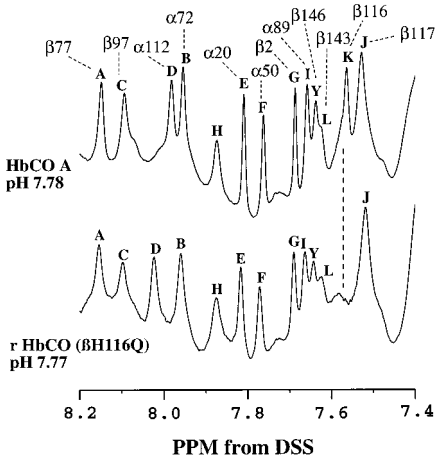

FIGURE 4: ^{1}H NMR spectra (500 MHz) of 2−6% solutions of rHbCO (βH116Q) and HbCO A in D_2O in 0.1 M HEPES at 29 °C.

nearly two decades, 2D TOCSY experiments also have been carried out to ensure the correctness of this assignment. Proton resonances belonging to the same amino acid residue form cross-peaks in the 2D TOCSY spectrum. Resonance T in the region of C4 proton resonances is also missing in the spectrum of rHbCO (βH143S) (Figure 2). Resonances L and T form a cross-peak in the 2D TOCSY spectrum of HbCO A (Figure 3), and this cross-peak does not appear in the spectrum of HbCO(βH143S) (result not shown). Thus, resonances L and T originate from the same histidyl residue, β143His.

The 500-MHz C2 proton resonances of the histidyl residues of rHbCO (βH116Q) and HbCO A in D_2O in 0.1 M HEPES buffer at 29 °C are shown in Figure 4. Resonance K is missing in the spectrum of rHbCO (βH116Q). Several other buffer conditions, such as different pH and the presence of chloride, also confirmed the absence of resonance K (results not shown). These lead to the assignment of C2 proton resonance K to β116His.

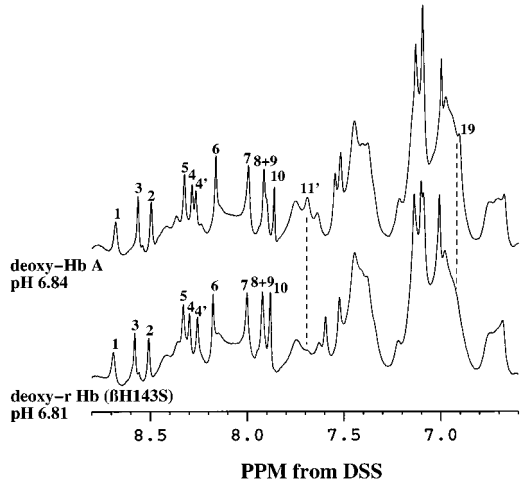

FIGURE 5: ^{1}H NMR spectra (600 MHz) of 2−6% solutions of deoxy-rHb(βH143S) and deoxy-Hb A in D_2O in 0.1 M HEPES plus 0.1 M NaCl at 29 °C.

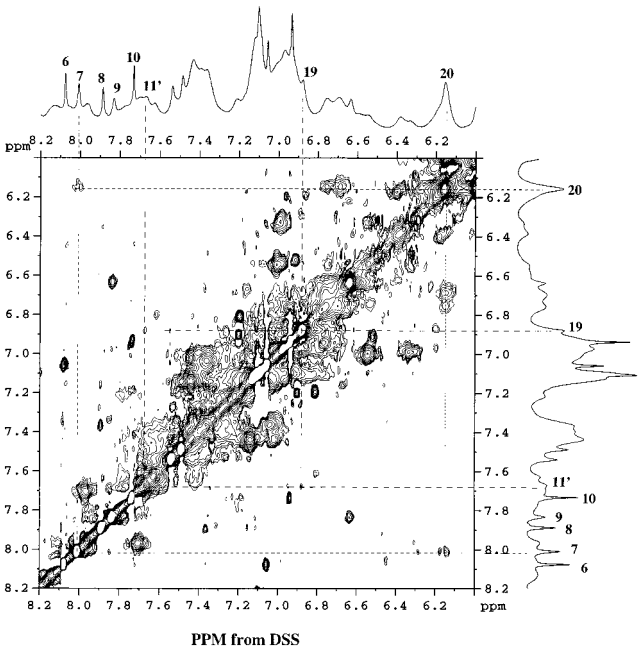

FIGURE 6: ^{1}H NMR TOCSY spectrum (600 MHz) of a 6% solution of deoxy-Hb A in D_2O in 0.1 M HEPES at pH 6.82 and 29 °C.

Assignment of the C2 Resonances of β116His and β143His in Deoxy-Hb A. Figure 5 shows the 600-MHz C2 and C4 proton resonances (∼8.8−7.6 ppm and ∼7.6−6.4 ppm from DSS, respectively) of the histidyl residues of deoxy-rHb-(βH143S) and deoxy-Hb A in D_2O in 0.1 M HEPES buffer plus 0.1 M chloride at 29 °C. The absence of resonance 11′ in the region of C2 proton resonances in the spectrum of deoxy-rHb(βH143S) has led to the assignment of resonance 11′ to β143His. We have confirmed this assignment in D_2O in 0.1 M HEPES buffer with and without chloride at several pH values ranging from 6.2 to 7.0 (results not shown). Resonance 11′ is a newly discovered resonance, since it is only resolved at the higher field, especially in the presence of chloride (Figures 5 and 6). 2D TOCSY experiments also have been carried out to confirm this assignment (Figure 6). Another resonance in the region of C4 proton resonances (labeled as 19 in the present study) is also missing from the spectrum of deoxy-rHb (βH143S) (Figure 5). Resonances 11′ and 19 belong to the same histidyl residue, β143His, as indicated by the presence of a cross-peak from these two resonances (Figure 6).

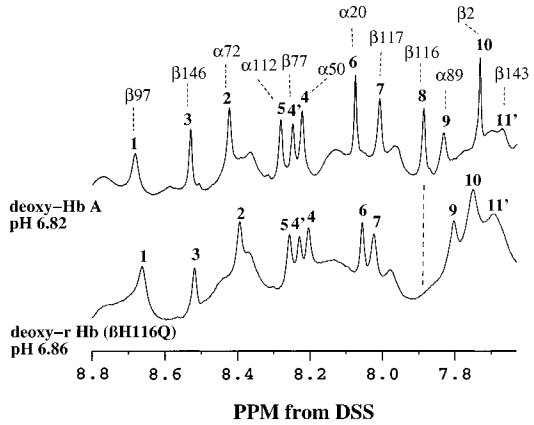

FIGURE 7: ^{1}H NMR spectra (600 MHz) of 2−6% solutions of deoxy-rHb(βH116Q) and deoxy-Hb A in D_2O in 0.1 M HEPES at 29 °C.

Figure 7 shows the C2 proton resonances of the histidyl residues of deoxy-rHb(βH116Q) and deoxy-Hb A in D_2O in 0.1 M HEPES buffer at 29 °C. The absence of resonance 8 in the spectrum of deoxy-rHb(βH116Q) leads to the assignment of resonance 8 to β116His. Several other buffer conditions, such as different pH and the presence of chloride, also have shown the absence of resonance 8 (results not shown). However, resonance 7 has been shifted downfield ∼0.1 ppm in the spectra of deoxy-rHb(βH116Q) in D_2O in 0.1 M HEPES buffer in the presence of 0.1 M chloride at 29 °C (results not shown). Since resonances 7 and 8 have been assigned to β116His and β117His in a previous study (*11*), resonance 7 should be assigned to β117His. The perturbation of resonance 7 is due to the fact that β116His and β117His are located next to each other in the structure. 2D TOCSY experiments also have provided evidence for these assignments. Figure 6 shows resonances 7 and 20 (assigned to the C4 proton resonance of β117His and labeled as 20 in this study) form a cross-peak at 8.01 and 6.16 ppm from DSS. Since the C4 proton of β117His is the closest distance to an aromatic ring (∼4.5 Å and outside the plane of the aromatic ring of β118Phe) among all the surface histidyl residues, it is very reasonable that the C4 proton of β117His has been shifted upfield to 6.16 ppm, which is not in the usual range of C4 proton resonances of surface histidyl residues. These confirm the assignments of C2 proton resonance 8 to β116His and resonance 7 to β117His.

pK Values of Surface Histidyl Residues in 0.1 M HEPES Buffer plus 0.1 M Chloride in D_2O. The 500- and 600-MHz ^{1}H NMR spectra of deoxy-Hb A and HbCO A in 0.1 M HEPES buffer plus 0.1 M chloride in D_2O, pH 4∼9, at 29 °C were used to determine the p*K* values of surface histidyl residues. The pH values of Hb A samples were titrated back and forth with 0.1 M HEPES-Na plus 0.1 M NaCl in D_2O or 0.1 M HEPES acid plus 0.1 M DCl in D_2O to different values. Although a very small amount of precipitation was noticed at lower pH (<5) values, the ^{1}H spectra of Hb A at higher pH values were still reproducible when we titrated those lower pH samples back to higher pH values. The chemical shifts of each C2 proton resonance have been fit as a function of pH to eq 1, and the results are presented in Table 1. Deviations from the protonation equilibrium as

Table 1: pK Values of Histidyl Residues in Deoxy-Hb A and HbCO A in 0.1 M HEPES plus 0.1 M Chloride in D_2O at 29 °C from a Nonlinear Least-Squares Fit of Experimental Data to Eq 1

resonance	site	pK	δ^+	δ^o
		deoxy-Hb A		
1	β97	8.01 ± 0.01	8.732 ± 0.002	7.615 ± 0.007
2	α72	7.41 ± 0.02	8.742 ± 0.008	7.637 ± 0.012
3	β146	7.81 ± 0.02	8.654 ± 0.004	7.776 ± 0.011
4	α50	7.12 ± 0.01	8.577 ± 0.005	7.720 ± 0.005
4′	β77	7.44 ± 0.01	8.459 ± 0.004	7.508 ± 0.006
5	α112	7.46 ± 0.01	8.458 ± 0.003	7.778 ± 0.006
6	α20	7.00 ± 0.02	8.548 ± 0.008	7.613 ± 0.008
7	β117	6.61 ± 0.06	8.591 ± 0.030	7.562 ± 0.022
8	β116	6.45 ± 0.04	8.435 ± 0.015	7.649 ± 0.011
9	α89	6.80 ± 0.01	8.415 ± 0.004	7.401 ± 0.003
10	β2	6.20 ± 0.02	8.560 ± 0.007	7.675 ± 0.004
11′	β143	4.69 ± 0.02	8.646 ± 0.016	7.670 ± 0.002
		HbCO A		
A	β77	7.73 ± 0.01	8.644 ± 0.002	7.673 ± 0.007
B	α72	7.27 ± 0.01	8.711 ± 0.002	7.742 ± 0.003
C	β97	7.66 ± 0.02	8.567 ± 0.004	7.716 ± 0.011
D	α112	7.48 ± 0.02	8.575 ± 0.004	7.686 ± 0.009
E	α20	7.06 ± 0.01	8.588 ± 0.005	7.674 ± 0.007
F	α50	6.90 ± 0.02	8.627 ± 0.008	7.676 ± 0.008
G	β2	6.41 ± 0.02	8.555 ± 0.008	7.676 ± 0.005
H	α45[a]	6.09 ± 0.02	8.629 ± 0.009	7.870 ± 0.004
I	α89	6.30 ± 0.03	8.328 ± 0.011	7.661 ± 0.006
J	β117	6.42 ± 0.03	8.535 ± 0.015	7.503 ± 0.009
K	β116	6.26 ± 0.04	8.394 ± 0.021	7.562 ± 0.011
L	β143	5.73 ± 0. 04	8.319 ± 0.017	7.648 ± 0.005
Y	β146	6.47 ± 0.04	8.473 ± 0.018	7.633 ± 0.011

[a] Resonance H was tentatively assigned to α45His in a previous study (*36*). Recently, our multinuclear, multidimensional NMR studies on ^{15}N-labeled rHb A together with our extensive ^1H NMR studies of the histidyl residues of Hb A have confirmed this assignment (Simplaceanu, Lukin, Fang, Zou, Ho, and Ho, unpublished results).

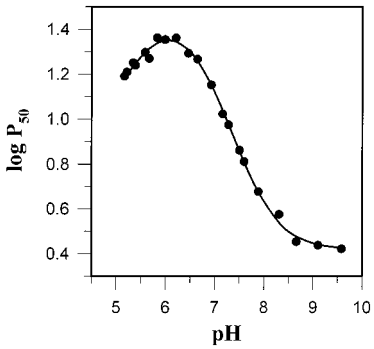

FIGURE 8: Oxygen dissociation data for Hb A in D_2O in 0.1 M HEPES plus 0.1 M NaCl at 29 °C presented as log P_{50} as a function of pH. The solid line represents the nonlinear least-squares fit of the data to the linkage equation as in a previous study (*8*).

predicted by the Henderson−Hasselbalch equation were determined by the fit of the data to eq 2, which includes the titration coefficient (n), as previously described (*8*). The results are presented in Table 2. The small value of n (i.e., $n < 1$) in Table 2 suggests that significant interactions with another ionizable group are taking place. A detailed discussion on this topic has been given previously (*8*).

Oxygen Dissociation and the Bohr Effect of Hb A in 0.1 M HEPES Buffer plus 0.1 M Chloride. Figure 8 shows the oxygen dissociation data presented as log P_{50} as a function of pH (pH 5−10). The log P_{50} data have been fit to the linkage equation given by Wyman (*4*) as in a previous study (*8*). The solid line in Figure 8 represents the nonlinear least-squares fit of the data to the linkage equation, resulting in four pK values: p$K_1' = 7.87$, p$K_1'' = 6.81$, p$K_2' = 4.79$, and p$K_2'' = 5.41$. The single prime refers to the deoxy

Table 2: pK Values of Histidyl Residues in Deoxy-Hb A and HbCO A in 0.1 M HEPES plus 0.1 M Chloride in D_2O at 29 °C from a Nonlinear Least-Squares Fit of Experimental Data to Eq 2

resonance	site	pK	δ^+	δ^o	n
			deoxy-Hb A		
1	β97	8.01 ± 0.01	8.731 ± 0.003	7.620 ± 0.014	1.01 ± 0.02
2	α72	7.47 ± 0.01	8.769 ± 0.004	7.547 ± 0.011	0.80 ± 0.01
3	β146	7.93 ± 0.02	8.674 ± 0.003	7.668 ± 0.015	0.79 ± 0.02
4	α50	7.14 ± 0.01	8.591 ± 0.003	7.689 ± 0.005	0.87 ± 0.01
4′	β77	7.46 ± 0.01	8.472 ± 0.003	7.471± 0.005	0.89 ± 0.01
5	α112	7.49 ± 0.01	8.466 ± 0.003	7.755 ± 0.008	0.90 ± 0.02
6	α20	7.02 ± 0.01	8.575 ± 0.004	7.555 ± 0.006	0.79 ± 0.01
7	β117	6.43 ± 0.07	8.885 ± 0.061	7.300 ± 0.052	0.40 ± 0.04
8	β116	6.35 ± 0.04	8.538 ± 0.017	7.553 ± 0.013	0.56 ± 0.03
9	α89	6.80 ± 0.01	8.421 ± 0.004	7.389 ± 0.005	0.95 ± 0.02
10	β2	6.17 ± 0.02	8.579 ± 0.009	7.663 ± 0.005	0.89 ± 0.03
11′	β143	4.70 ± 0.05	8.638 ± 0.042	7.670 ± 0.002	1.01 ± 0.05
			HbCO A		
A	β77	7.79 ± 0.01	8.657 ± 0.001	7.607 ± 0.005	0.87 ± 0.01
B	α72	7.27 ± 0.01	8.715 ± 0.002	7.734 ± 0.003	0.97 ± 0.01
C	β97	7.75 ± 0.02	8.587 ± 0.004	7.633 ± 0.018	0.81 ± 0.03
D	α112	7.53 ± 0.01	8.598 ± 0.004	7.622 ± 0.011	0.83 ± 0.02
E	α20	7.08 ± 0.01	8.616 ± 0.003	7.631 ± 0.004	0.84 ± 0.01
F	α50	6.90 ± 0.02	8.650 ± 0.009	7.648 ± 0.011	0.88 ± 0.03
G	β2	6.39 ± 0.01	8.587 ± 0.009	7.654 ± 0.005	0.86 ± 0.02
H	α45[a]	6.12 ± 0.02	8.606 ± 0.009	7.880 ± 0.004	1.14 ± 0.04
I	α89	6.25 ± 0.03	8.368 ± 0.016	7.644 ± 0.008	0.82 ± 0.05
J	β117	6.39 ± 0.02	8.596 ± 0.018	7.458 ± 0.012	0.78 ± 0.03
K	β116	6.13 ± 0.05	8.537 ± 0.031	7.491 ± 0.014	0.62 ± 0.04
L	β143	5.57 ± 0. 06	8.427 ± 0.030	7.622 ± 0.006	0.71 ±0.04
Y	β146	6.42 ± 0.03	8.581 ± 0.019	7.546 ± 0.013	0.63 ±0.03

[a] Resonance H was tentatively assigned to α45His in a previous study (*36*). Recently, our multinuclear, multidimensional NMR studies on ^{15}N-labeled rHb A together with our extensive ^1H NMR studies of the histidyl residues of Hb A have confirmed this assignment (Simplaceanu, Lukin, Fang, Zou, Ho, and Ho, unpublished results).

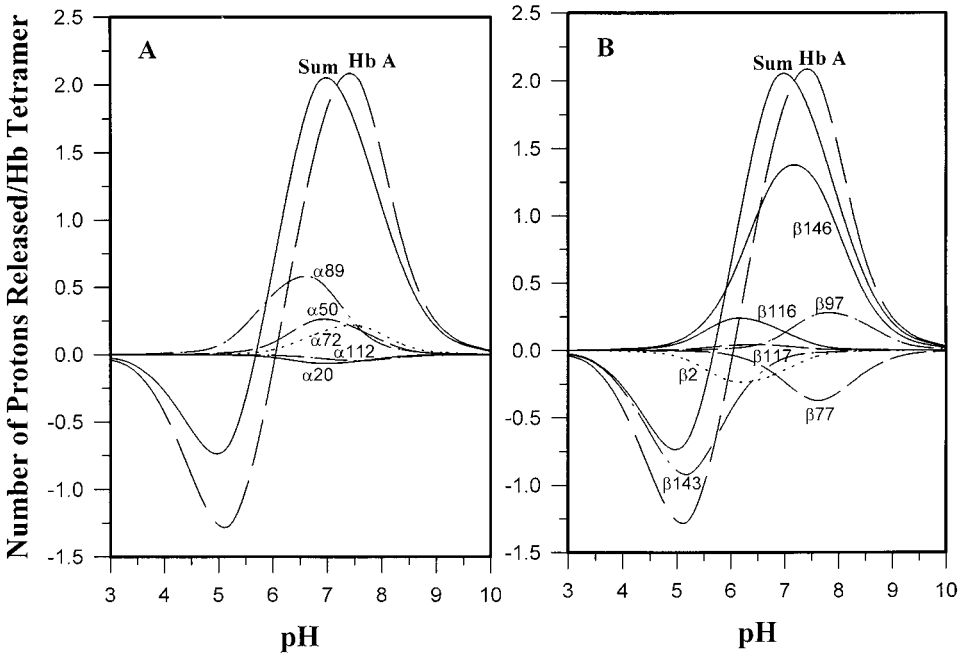

FIGURE 9: Bohr effect of Hb A in D_2O in 0.1 M HEPES plus 0.1 M NaCl at 29 °C. The Bohr effect of Hb A is determined from oxygen dissociation studies. The contributions from individual histidyl residues are calculated by using the p*K* values listed in Table 2. Sum is the summation of the contributions from all 24 surface histidyl residues.

conformation (T state), and the double prime refers to the oxy conformation (R state). The oxygenation cooperativity is maintained well over the entire pH range, since the cooperativity values calculated from the individual oxygen dissociation curves range from 2.3 to 3.1 under these conditions. Therefore, the Bohr effect, expressed as the number of H^+ ions released per Hb tetramer (ΔH^+) upon oxygenation (from T state to R state) as a function of pH, can be calculated as in a previous study (*8*). The Bohr effect of Hb A in D_2O in 0.1 M HEPES buffer plus 0.1 M chloride at 29 °C is plotted in Figure 9. By use of the p*K* values derived from NMR studies, the contribution from individual surface histidyl residues is calculated as in a previous study (*18*). The contributions from individual surface histidyl residues and their sum are also plotted in Figure 9. The comparison in Figure 9 reveals the contribution of individual surface histidyl residues to the net Bohr effect of Hb A. The sum of contributions of these 24 surface histidyl residues does not account for all of the measured Bohr effect for Hb A.

Effect of 2,3-BPG on the C2 Proton Resonances of the Histidyl Residues in Hb A and rHb(βH143S). The C2 proton resonances of the histidyl residues of Hb A and rHb (*β*H143S) in the absence or presence of 2,3-BPG (2:1 molar ratio to Hb) are shown in Figure 10. The addition of 2,3-BPG to Hb A solutions specifically affects several resonances in both the deoxy and CO forms as shown in a previous study (*22*). In the CO form, the addition of 2,3-BPG to Hb A solutions results in resonances G and Y (assigned to *β*2His and *β*146His, respectively) being shifted downfield by 0.03−0.04 ppm and resonance L (assigned to *β*143His) being broadened beyond detection. In the deoxy form, resonances 10 and 11′ (assigned to *β*2His and *β*143His, respectively) in the spectra of Hb A are shifted downfield by 0.2 and 0.05 ppm, respectively, in the presence of 2,3-BPG. In the spectra of rHb (*β*H143S), the addition of 2,3-BPG still results in similar changes for resonances G, Y, and 10. These results

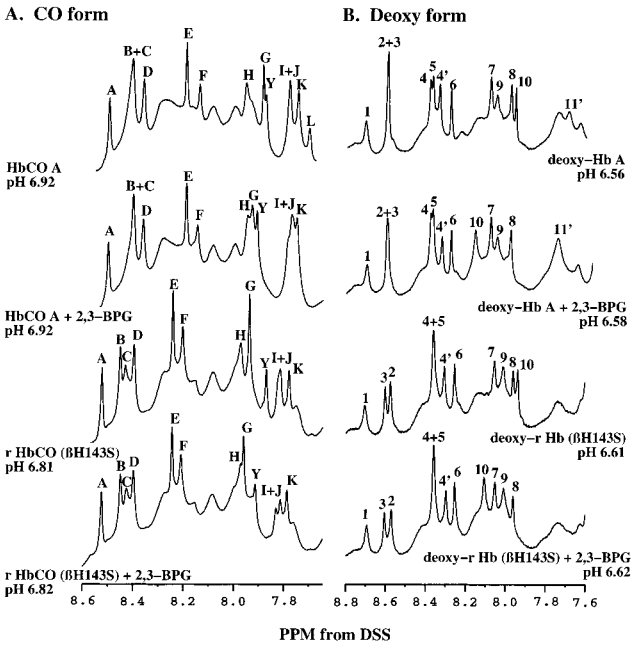

FIGURE 10: ^1H NMR spectra (600 MHz) of 2−6% solutions of rHb (*β*H143S) and Hb A in D_2O in 0.1 M HEPES plus 0.1 M NaCl at 29 °C: (A) CO form and (B) deoxy form. Effects of 2,3-BPG (2:1 molar ratio to Hb) upon the C2 proton resonances are shown.

indicate that rHb (*β*H143S) still can bind 2,3-BPG.

Oxygen-Binding Properties of Hb A, Hb F, and rHb-(βH143S). The oxygen-binding properties of Hb A, Hb F, and rHb (*β*H143S) are summarized in Figure 11 and Table 3. 2,3-BPG and inositol hexaphosphate (IHP), a much stronger allosteric effector than 2,3-BPG, are also used to study the oxygen-binding properties of these Hbs. In 0.1 M sodium phosphate buffer at 29 °C, rHb (*β*H143S) exhibits slightly higher oxygen affinity and a smaller Hill coefficient (n_{max}) than Hb A over the entire pH range studied. In general, all of these Hbs have lowered oxygen affinity due to the

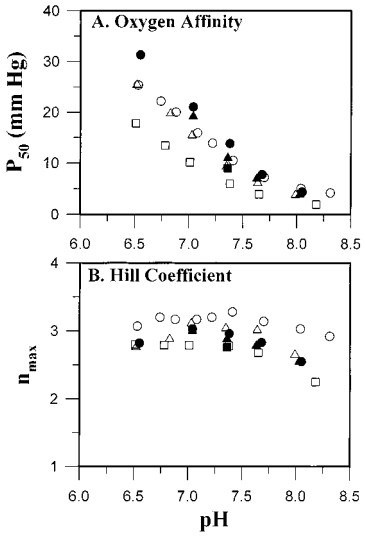

FIGURE 11: pH dependence of oxygen affinity (A) and the Hill coefficient (B): (○) Hb A; (●) Hb A with 5 mM 2,3-BPG; (△) Hb F; (▲), Hb F with 5 mM 2,3-BPG; (□) rHb (βH143S); (■) rHb (βH143S) with 5 mM 2,3-BPG. P_{50} and n_{max} were determined from each oxygen dissociation curve. Oxygen dissociation curves were obtained with 0.1 mM Hb in 0.1 M sodium phosphate buffer in the pH range 6.5−8.5 at 29 °C.

Table 3: P_{50} and n_{max} Values for Hb A, Hb F, and rHb(βH143S) in the Presence and Absence of 2,3-BPG or IHP[a]

	P_{50} (mmHg)			n_{max}		
	none	5 mM 2,3-BPG	1 mM IHP	none	5 mM 2,3-BPG	1 mM IHP
Hb A	8.2	13.8	32.0	3.1	3.0	2.6
Hb F	9.4	11.0	15.4	3.0	2.9	2.9
rHb(βH143S)[b]	6.0	9.0	26.6	2.8	2.8	2.9

[a] Data were obtained with 0.1 mM Hb in 0.1 M sodium phosphate buffer at pH 7.4 and 29 °C. [b] The oxygen binding properties of rHb (βH143S) were measured in the presence of a reductase system (*32*) to reduce the amount of the met-Hb formed to less than 5% during the oxygenation process.

presence of 2,3-BPG or IHP (Figure 11 and Table 3). In the presence of 5 mM 2,3-BPG, the P_{50} values increased 68%, 18%, and 50% for Hb A, Hb F, and rHb (βH143S), respectively. In the presence of 1 mM IHP, the P_{50} values increased 288%, 65%, and 342% for Hb A, Hb F, and rHb (βH143S), respectively (Table 3). In comparison with Hb A, the slightly lower oxygen affinity of Hb F in the absence of 2,3-BPG and the insensitivity of Hb F to 2,3-BPG are consistent with the results obtained previously (*37*−*39*). The results for rHb (βH143S) suggest that this mutant still binds 2,3-BPG and IHP quite well and both phosphates exert a strong influence on the oxygen-binding properties of this rHb.

DISCUSSION

In this study, we have assigned resonances K and 8 to β116His, and resonances L and 11′ to β143His. A previous study on Hb A_2 (*11*) assigned resonances J, K, 7, and 8 to β116 and β117 histidine residues; however, the individual assignments for these two histidine residues were not specified. The assignment of resonances K and 8 to β116His has led to the assignment of resonances J and 7 to β117His indirectly. In the past, the assignments for β97His and β143His have been controversial. Resonance C has been assigned to β97His by some researchers and to β143His by other researchers (*13*, *15*, *16*). The present assignment of resonance L to β143His has led to the correct assignment of resonance C to β97His. Since β143His is involved in the binding of 2,3-BPG, the present assignment of resonance L to β143His is also consistent with the fact that resonance L is broadened beyond detection in the presence of 2,3-BPG (Figure 10) (*3*, *22*). On the basis of previous and present ^{1}H NMR studies, the assignments for 24 surface histidyl residues per tetramer or 12 surface histidyl residues per $\alpha\beta$ dimer are listed in Tables 1 and 2. In this work, we have completed the resonance assignments for surface histidyl residues of Hb A.

The oxygen affinity of Hb A in 0.1 M HEPES buffer plus 0.1 M chloride in D_2O at 29 °C has been determined in this study. The calculated maximum number of H^+ ions released from Hb A upon oxygenation is 2.1 mol/mol of tetramer at pH 7.4. The calculated maximum number of H^+ ions taken up by Hb A upon oxygenation is 1.3 mol/mol of tetramer at pH 5.1 (Figure 9). These data are very close to the data of Hb A in Bis-Tris or Tris buffer with 0.1 M NaCl determined by Matsukawa et al. (*12*) either by the direct differential titration method or by the measurement of oxygen affinity as a function of pH. The p*K* values of surface histidyl residues in 0.1 M HEPES buffer plus 0.1 M chloride in D_2O at 29 °C also have been determined in this study (Table 2). These p*K* values are very similar to those determined in 0.1 M Bis-Tris buffer plus 0.18 M NaCl in D_2O at 29 °C in a previous study (*7*). Here, we have also determined the p*K* values for resonances 11′ (which comes from β143His) and Y (which belongs to β146His) that have not been determined previously. β146His and β143His have the largest decrease and increase, respectively, in their p*K* values in going from deoxy to CO forms. α20His, α112His, and α117His have no changes; α50His, α72His, α89His, β97His, and β116His have moderate decreases; and β2His and β77His have moderate increases in their p*K* values in going from deoxy to CO forms (Table 2). The larger the decrease in the p*K* values, the bigger is the positive contribution to the Bohr effect. In contrast, the larger the increase in the p*K* values, the bigger is the negative contribution to the Bohr effect (Table 2 and Figure 9). Among the surface histidyl residues, β146His has the biggest contribution to the alkaline Bohr effect (63% at pH 7.4), and β143His has the biggest contribution to the acid Bohr effect (71% at pH 5.1). The importance of the β146His residue to the alkaline Bohr effect of Hb A has been discussed previously (*8*). The sum of the contributions from 24 surface histidyl residues is 86% of the alkaline Bohr effect at pH 7.4 and is 55% of the acid Bohr effect at pH 5.1. This leaves 14% of the alkaline Bohr effect (at pH 7.4) and 45% of the acid Bohr effect (at pH 5.1) unaccounted for in 0.1 M HEPES buffer with 0.1 M chloride.

We have mentioned earlier that any amino acid residue that changes its p*K* values between the deoxy and oxy (or CO) forms of the Hb molecule participates in the Bohr effect. Some amino acid residues that have differential affinities for anions between the deoxy and oxy (or CO) states are also potential Bohr groups. In addition to the surface histidyl residues, the p*K* values of the side-chain γ-carboxyl group of β43Glu have been reported to change significantly from deoxy (7.0) to oxy (6.35) form (*40*). The p*K* values of the

α-amino group of α1Val have also been reported to decrease from 7.8 to 7.3 upon oxygenation (*41*). de Bruin et al. (*42*) have proposed that the anion composition is an important regulating factor of the Bohr effect. Since the determination of the p*K* values for *β*43Glu and α1Val were not carried out in the same solvent conditions as in this study, we feel that it is not appropriate to bring these two residues into our calculation for the Bohr effect. It is possible that these two amino acid residues can account for the rest of the 14% of the alkaline Bohr effect in 0.1 M HEPES buffer with 0.1 M chloride at pH 7.4. In addition to the histidine residues, aspartate and glutamate residues may also contribute to the acid Bohr effect; however, the lack of a simple and direct method to determine the p*K* values of these amino acid residues makes their identification very difficult.

The current study plus other previous studies show that 22 amino acid residues—18 of the surface histidyl residues, two α1Val, and two *β*43Glu—contribute to the Bohr effect. As suggested previously (*18*), the heterotropic interaction depends on the intricate arrangement and interactions of all proton binding sites in Hb. The results in this study strongly support the idea that the global network of electrostatic interactions plays a dominant role in the Bohr effect of Hb (*18*).

According to crystal structure and ^{31}P NMR studies, *β*143His is involved in the binding of 2,3-BPG to Hb A. The insensitivity of Hb F to 2,3-BPG and the lack of a histidyl residue in position 143 of the *γ*-chain suggested an important role for *β*143His in the binding of 2,3-BPG to Hb A. However, we find that the binding of 2,3-BPG with rHb (*β*H143S) and the binding with Hb A are very similar on the basis of our ^{1}H NMR results and oxygen binding studies. Since the p*K* values for *β*143His are quite low (4.7 and 5.6 in deoxy and CO forms of Hb A, respectively), the salt bridge between *β*143His and 2,3-BPG should be very weak in the neutral pH range. *β*2His has higher p*K* values (6.2 and 6.4 in deoxy and CO forms of Hb A, respectively) than *β*143His; therefore, the salt bridge between *β*2His and 2,3-BPG should be stronger than that between *β*143His and 2,3-BPG. This suggestion is also consistent with the fact that resonances 10 and G (assigned to *β*2His) show the biggest change among the C2 resonances in ^{1}H NMR spectra of deoxy-Hb A and HbCO A, when 2,3-BPG is added. Therefore, the other differences between the *β*- and *γ*-chains may play a more significant role in the insensitivity of Hb F to 2,3-BPG. Despite 39 residues of the amino acid sequences of the *β*- and *γ*-chains being different, the crystal structures of human deoxy-Hb F and deoxy-Hb A have shown that the only detectable differences in the tertiary structures between *β*- and *γ*-chains appear in the two N-terminal segments (*43*). Because of the shift of the N-terminus, an anion bound between *β*1Val and *β*82Lys in deoxy-Hb A is absent from deoxy-Hb F, and the distance between the two phosphate groups of 2,3-BPG and *β*2His may be increased in deoxy-Hb F. Frier and Perutz (*43*) suggested that a shift of the N-terminus due to the substitution *β*3Leu to *γ*3Phe might contribute to the lower affinity of deoxy-Hb F for 2,3-BPG.

The higher oxygen affinity of rHb (*β*H143S) in the absence of 2,3-BPG from pH 7.4 to 8.2 is unexpected (Table 3 and Figure 11). Oxygen binding experiments have been carried out to determine whether this higher oxygen affinity is caused by the intrinsically high oxygen affinity in the absence of an anion or by the decreased anion effect on oxygen affinity as compared to Hb A. The P_{50}s of Hb A are 2.8, 3.2, and 7.3 mmHg in 0.1 M HEPES with 0, 0.002, and 0.1 M NaCl, respectively, at pH 7.4 and 29 °C. The P_{50}s of rHb (*β*H143S) are 2.3 and 5.2 mmHg in 0.1 M HEPES with 0.002 and 0.1 M NaCl, respectively, at pH 7.4 and 29 °C. However, the intrinsic oxygen affinity obtained in the absence of chloride is not available for rHb (*β*H143S) due to 8.3% met-Hb formed during the oxygenation process. The met-Hb formation during the oxygenation process is a general problem for many genetically engineered mutations or chemical modifications with a functional change. As we mentioned earlier, a met-Hb reductase system was used if needed to reduce the amount of met-Hb formed to less than 5% during the oxygenation process (*32*). Imaizumi et al. (*44*) reported that the oxygen binding properties of Hb A are affected, however, by the presence of the met-Hb reductase system at chloride concentration ≤0.03 M, presumably due to the presence of the glucose 6-phosphate and nicotinamide adenine dinucleotide in the reductase system. Therefore, we cannot apply the met-Hb reductase system to obtain the intrinsic oxygen affinity of rHb (*β*H143S). The intrinsic oxygen affinity of rHb (*β*H143S) obtained in the absence of chloride should be either the same or higher than that obtained in the presence of 0.002 M NaCl. Therefore, the intrinsic oxygen affinity of rHb (*β*H143S) in the absence of chloride should be higher than that of Hb A. The chloride effect on the oxygen affinity of Hb A and rHb (*β*H143S) was estimated from the increase of the P_{50} values in the presence of 0.002 M−0.1 M chloride. The P_{50} values obtained in the presence of 0.1 M chloride increased 128% and 125% for Hb A and rHb (*β*H143S), respectively, compared to those obtained in the presence of 0.002 M chloride. Thus, the anion effect is not responsible for the observed higher oxygen affinity of rHb (*β*H143S). As we have mentioned earlier, *β*143His is located in the central cavity of the Hb molecule. The excess positive charge in the central cavity is suggested to play an important role in the oxygen binding of the Hb molecules (*45*−*47*). Perutz et al. (*45*, *46*) suggested that introducing additional positive charge(s) into the central cavity should destabilize the T-structure and therefore increase the oxygen affinity, while introducing negative charge(s) or removing positive charge(s) should have the opposite effect. In addition to rHb Presbyterian (*β*N108K) (*31*), our rHb (*β*H143S) does not follow the above mechanism. However, Perutz et al. (*46*) did point out a few exceptions to the above mechanism, such as Hb Little Rock (*β*H143Q) and Hb Syracuse (*β*H143P). They suggested that the increased oxygen affinity may be due to the disrupting effect of these mutations on the essential C-terminal salt bridge of the *β*-chain in the T-structure (*48*). This suggestion might also explain the higher oxygen affinity of rHb (*β*H143S) compared to that of Hb A.

In conclusion, a global network of electrostatic interactions plays a dominant role in the Bohr effect of Hb. We have accurately measured and assigned the individual p*K* values for all surface histidyl residues in Hb A. The sum of the contributions from 24 surface histidyl residues accounts for 86% of the alkaline Bohr effect at pH 7.4 and about 55% of the acid Bohr effect at pH 5.1. With the accurately measured and assigned individual p*K* values for all surface histidyl residues, it is now possible to evaluate the Bohr effect

microscopically for novel recombinant Hbs with important functional properties, such as low oxygen affinity and high cooperativity. β143His is not important to the alkaline Bohr effect; it mainly contributes to the acid Bohr effect. In addition, β143His is not essential for the binding of 2,3-BPG to Hb A in the neutral pH range.

ACKNOWLEDGMENT

We thank Dr. Ming F. Tam for carrying out electrospray ionization mass spectrometric analyses and Edman degradation experiments to evaluate the quality of the recombinant hemoglobins used in this study. We also thank Dr. E. Ann Pratt for helpful comments on our manuscript.

REFERENCES

1. Benesch, R. E., Benesch, R., and Yu, C. I. (1969) *Biochemistry 8*, 2567−2571.
2. Antonini, E., and Brunori, M. (1971) *Hemoglobin and Myoglobin in Their Reactions with Ligands*, North-Holland, Amsterdam.
3. Busch, M. R., and Ho, C. (1990) *Biophys. Chem. 37*, 313−322.
4. Wyman, J. (1948) *Adv. Protein Chem. 4*, 407−531.
5. Wyman, J. (1964) *Adv. Protein Chem 19*, 223−286.
6. Russu, I. M., Ho, N. T., and Ho, C. (1980) *Biochemistry 19*, 1043−1052.
7. Russu, I. M., Wu, S. S., Ho, N. T., Kellogg, G. W., and Ho, C. (1989) *Biochemistry 28*, 5298−5306.
8. Busch, M. R., Mace, J. E., Ho, N. T., and Ho, C. (1991) *Biochemistry 30*, 1865−1877.
9. Kilmartin, J. V., Breen, J. J., Roberts, G. C., and Ho, C. (1973) *Proc. Natl. Acad. Sci. U.S.A. 70*, 1246−1249.
10. Russu, I. M., Ho, N. T., and Ho, C. (1982) *Biochemistry 21*, 5031−5043.
11. Russu, I. M., Lin, A. K., Ferro-Dosch, S., and Ho, C. (1984) *Biochim. Biophys. Acta 785*, 123−131.
12. Matsukawa, S., Itatani, Y., Mawatari, K., Shimokawa, Y., and Yoneyama, Y. (1984) *J. Biol. Chem. 259*, 11479−11486.
13. Perutz, M. F., Gronenborn, A. M., Clore, G. M., Fogg, J. H., and Shih, D. T. (1985) *J. Mol. Biol. 183*, 491−498.
14. Perutz, M. F., Gronenborn, A. M., Clore, G. M., Shih, D. T., and Craescu, C. T. (1985) *J. Mol. Biol. 186*, 471−473.
15. Craescu, C. T., Schaeffer, C., Mispelter, J., Garin, J., and Rosa, J. (1986) *J. Biol. Chem. 261*, 7894−7901.
16. Russu, I. M., and Ho, C. (1986) *Biochemistry 25*, 1706−1716.
17. Ho, C., and Russu, I. M. (1987) *Biochemistry 26*, 6299−6305.
18. Sun, D. P., Zou, M., Ho, N. T., and Ho, C. (1997) *Biochemistry 36*, 6663−6673.
19. Dickerson, R. E., and Geis, I. (1983) *Hemoglobin: Structure, Function, Evolution, and Pathology*, Benjamin/Cummings, Menlo Park, CA.
20. Perutz, M. F. (1970) *Nature 228*, 726−739.
21. Baldwin, J. M. (1980) *J. Mol. Biol. 136*, 103−128.
22. Russu, I. M., Wu, S. S., Bupp, K. A., Ho, N. T., and Ho, C. (1990) *Biochemistry 29*, 3785−3792.
23. Benesch, R. E., and Benesch, R. (1974) *Adv. Protein Chem. 28*, 211−237.
24. Arnone, A. (1972) *Nature 237*, 146−148.
25. Gupta, R. K., Benovic, J. L., and Rose, Z. B. (1979) *J. Biol. Chem. 254*, 8250−8255.
26. Shen, T. J., Ho, N. T., Simplaceanu, V., Zou, M., Green, B. N., Tam, M. F., and Ho, C. (1993) *Proc. Natl. Acad. Sci. U.S.A. 90*, 8108−8112.
27. Lindstrom, T. R., and Ho, C. (1972) *Proc. Natl. Acad. Sci. U.S.A. 69*, 1707−1710.
28. Kim, H. W., Shen, T. J., Sun, D. P., Ho, N. T., Madrid, M., Tam, M. F., Zou, M., Cottam, P. F., and Ho, C. (1994) *Proc. Natl. Acad. Sci. U.S.A. 91*, 11547−11551.
29. Kim, H. W., Shen, T. J., Sun, D. P., Ho, N. T., Madrid, M., and Ho, C. (1995) *J. Mol. Biol. 248*, 867−882.
30. Kim, H. W., Shen, T. J., Ho, N. T., Zou, M., Tam, M. F., and Ho, C. (1996) *Biochemistry 35*, 6620−6627.
31. Tsai, C. H., Shen, T. J., Ho, N. T., and Ho. C. (1999) *Biochemistry 38*, 8751−8761.
32. Hayashi, A., Suzuki, T., and Shih, M. (1973) *Biochim. Biophys. Acta 310*, 309−316.
33. Plateau, P., and Guéron, M. (1982) *J. Am. Chem. Soc. 104*, 7310−7311.
34. Bax, A., and Davis, D. G. (1985) *J. Magn. Reson. 65*, 355−360.
35. Ho, C. (1992) *Adv. Protein Chem. 43*, 153−312.
36. Ho, C., and Russu, I. M. (1985) *New Methodologies in Studies of Protein Configuration*, pp 1−35. Van Nostrand-Reinhold, New York.
37. Bunn, H. F., and Forget, B. G. (1986*) Hemoglobin: Molecular, Genetic and Clinical Aspects*, W. B. Saunders, Philadelphia, PA.
38. Giardina, B., Scatena, R., Clementi, M. E., Cerroni, L., Nuutinen, M., Brix, O., Sletten, S. N., Castagnola, M., and Condò, S. G. (1993) *J. Mol. Biol. 229*, 512−516.
39. Adachi, K., Konitzer, P., Pang, J., Reddy, K. S., and Surrey, S. (1997) *Blood 90*, 2916−2920.
40. Rao, M. J., and Acharya, A. S. (1992) *Biochemistry 31*, 7231−7236.
41. Kilmartin, J. V., and Rossi-Bernardi, L. (1973) *Physiol. Rev. 53*, 836−890.
42. de Bruin, S. H., Boen, F. J., Rollema, H. S., and van Beek, G. G. (1977) *Biophys. Chem. 7*, 169−172.
43. Frier, J. A., and Perutz, M. F. (1977) *J. Mol. Biol. 112*, 97−112.
44. Imaizumi, K., Ima, K., and Tyuma, I. (1979) *J. Biochem. (Tokyo) 86*, 1829−1840.
45. Perutz, M. F., and Fermi, G. (1993) *J. Mol. Biol. 233*, 536−545.
46. Perutz, M. F., Shih, D. T.-b., and Williamson, D. (1994) *J. Mol. Biol. 239*, 555−560.
47. Bonaventura, C., Arumugam, M., Cashon, R., Bonaventura, J., and Moo-Penn, W. F. (1994) *J. Mol. Biol. 239*, 561−568.
48. Perutz, M. F., Kilmartin, J. V., Nishikura, K., Fogg, J. H., Butler, P. J. G., and Rollema, H. S. (1980) *J. Mol. Biol. 138*, 649−670.

BI9911379